A Novel Structural Assessment Technique to Prevent Damaged FRP-Wrapped Concrete Bridge Piers from Collapse

Oral Büyüköztürk*

Department of Civil and Environmental Engineering

Massachusetts Institute of Technology

77 Mass. Ave., Room 1-280

Cambridge, Massachusetts 02139
U.S.A.
Email: obuyuk@mit.edu

Tzu-Yang Yu

Department of Civil and Environmental Engineering

Massachusetts Institute of Technology

77 Mass. Ave., Room 5-336

Cambridge, Massachusetts 02139
U.S.A.
Email: youngyu@mit.edu

Table of Content

Abstract

Repairing deteriorated concrete bridge piers using externally wrapped FRP (fiber reinforced polymer) composites has been proven as an effective approach. This technique has also been applied to low-rise building structures. Failures in FRP-wrapped concrete structures may occur by flexural failures of critical sections or by debonding of FRP plate from the concrete substrate. Debonding in the FRP/adhesive/concrete interface region may cause a significant decrease in member capacity leading to a premature failure of the system. In this paper, a novel structural assessment technique aiming at inspecting the near-surface FRP debonding and concrete cracking of damaged FRP-wrapped concrete bridge piers to prevent the structures from collapse is presented. In the first part of this paper, failure mechanisms of FRP-wrapped concrete systems are briefly discussed. The second part of this paper introduces a novel structural assessment technique in which far-field airborne radar is applied. In this development, emphasis is placed on inspection of debonding in glass FRP (GFRP)-wrapped concrete cylinders, while the technique is also applicable to beams and slabs with bonded GFRP composites. Physical radar measurements on laboratory specimens with structural damages were conducted and used for validating the technique. Processed experimental measurements have shown promising results for the future application of the technique. Finally, research findings and issues are summarized.

1. Introduction

Strengthening and repair of concrete structures has become an important issue for public safety and for effective infrastructure management. Engineering technologies are developed and introduced for extending the service life of concrete structures by means of restoring their design capacity for continuous use and/or upgrading them for possible future challenges from the environment. The use of fiber reinforced polymer (FRP) composites as an externally bonded element to confine the concrete in order to secure the integrity of concrete structures has been proven, both theoretically and practically, to be an effective strengthening/repair approach. FRP composite jacketing systems have emerged as an alternative to traditional construction, strengthening, and repair of reinforced concrete columns and bridge piers. A large number of projects, both public and private, have used this technology and escalating deployment is expected, especially in seismically active regions. Integration of the new FRP composite with the existing concrete substrate results in the formation of a new structural system. Differences in the material properties of the two structural components (FRP and concrete) pose challenging problems of predicting the behavior of the integrated structural system. Extensive research effort has been devoted to this

active field as reported in the literature on structural engineering, and composite materials and construction.

The integration of concrete structures with externally bonded GFRP composites forms a multi-layer composite system. Construction defects and structural/environmental damages may occur within the GFRP-retrofitted concrete structures, and especially, in the vicinity of FRP-concrete interfaces. FRP-concrete interface and concrete conditions cannot be fully revealed until physical removal of the FRP composite layer unless the member has already been subjected to apparent substantive damage. Partial or complete removal of the FRP composite layer for observation of the damage may pose a danger of structural collapse. It has been identified recently that a FRP-retrofitted beam or concrete column could appear safe without showing any sign of substantial damage underneath FRP composites and yet containing a severely deteriorated concrete and debonded FRP composites. Such scenario could happen when the structure has undergone a modest seismic event that has significantly damaged the FRP-concrete system while the system has not reached the failure stage. Failures of damaged FRP-concrete systems are often brittle, involving delamination of the FRP, debonding of concrete layers, and shear collapse, and can occur at load levels lower than the predicted theoretical strength of the retrofit system. Among these failure modes are fracture of concrete along the planes in the vicinity of FRP-adhesive interfaces, debonding or peeling of the FRP from the concrete surface due to the mechanical and environmental effects, and epoxy decohesion. Gradual debonding of the FRP composite under service load conditions may result in premature failures of the retrofitted system, leading to the total collapse of the structure. Thus, there is a need for inspection of debonding in such multi-layer systems using appropriate nondestructive testing (NDT) techniques applicable in field conditions. This is essential for safe applications of FRP strengthening of deteriorated concrete structures in prevention of total collapse.

In this paper, first the various failure mechanisms of debonding in FRP-wrapped concrete systems are discussed. The paper then focuses on the NDT techniques for the inspection of FRP-wrapped concrete systems. A novel NDT technique based on the far-field radar measurements developed by the authors is discussed as a structural assessment tool to prevent damaged GFRP-wrapped concrete structures from total collapse. In this development, emphasis is placed on inspection of debonding in GFRP-wrapped concrete bridge piers. Radar measurements are conducted on laboratory cylinder specimens with structural damages. Measurement results are provided and processed by the image reconstruction algorithm to render images for condition assessment.

2. Failure Mechanisms of FRP-wrapped Concrete Systems

Failures in FRP-wrapped concrete or reinforced concrete systems may occur by flexural failures of critical sections, such as FRP rupture and crushing of compressive concrete, or by debonding of FRP plate from the RC beams, both triggered by the presence of construction defects and structural damages. Construction defects such as trapped air voids or pockets can occur between FRP sheets/plates and concrete substrate during construction. Under mechanical effects stress concentrations would develop around such regions, leading to further development of delamination in the interface region and debonding of FRP from the concrete substrate. Structural damages such as concrete cracking or crumbling inside the FRP wrapping, and/or debonding of the FRP sheet from concrete could occur under various degrees of confinement pressure provided by the FRP wrap. This type of failure has been observed in FRP-wrapped concrete specimens [1], and also FRP-wrapped large scale reinforced concrete structures [2]. In addition, environmental (moisture) effects have been shown to lead to debonding [3]. Various approaches on the modeling of debonding have been proposed, such as strength approach, semi-empirical and empirical models, and fracture approach [4 ~ 6]. The presence of these defects and damages can initiate the brittle failure of FRP-strengthened concrete structures.

FRP debonding occurs with a loss in the confinement action between the bonded FRP and the RC member. Experimental results have shown that FRP debonding is a highly complex phenomenon that can involve failure propagation within the concrete substrate, within the adhesive, within the FRP laminate, and the interfaces of these layers [4, 7, 8]. It is possible that high stress concentrations around flexural cracks may promote debonding [9], however, such stress concentrations diminish rapidly with propagation of debonding, resulting in a certain debonded area. Durability of the FRP-strengthened RC system remains a major concern in rehabilitation applications. Behavior of FRP-strengthened RC systems subjected to freeze-thaw, wet-dry, and temperature variation cycles or various aqueous solutions prior to loading have been studied by researchers and varying degrees of strength degradation have been observed [10 ~ 15]. The influence of moisture on the adhesive is believed to play a critical role in the debonding failure of FRP/adhesive/concrete systems. The plasticization effect of moisture enhances the fracture toughness of adhesives due to greater plastic deformation and enhanced crack-tip blunting mechanisms [16]. Cohesive strength may, however, be reduced [17, 18] to sufficiently offset the increased toughness. These results show that durability is an important issue in FRP/adhesive/concrete systems.

3. Structural Assessment Technique – Far-field Airborne Radar NDT

In this section, a novel structural assessment technique called FAR (far-field airborne radar) NDT is described for the inspection of GFRP debonding, as the precursor of structural failures, in GFRP-concrete systems. Current NDT techniques are first reviewed. Compared to other NDT techniques such as acoustic NDT, thermal NDT, and radiography NDT, radar (electromagnetic wave) NDT is promising in field applications; the method is less vulnerable to temperature variation, and less constrained in field installation. While most current radar or microwave NDT adopt near-field inspection scheme [19], the developed FAR NDT technique uses far-field inspection scheme allowing inspections from distance for highway and cross-river bridge piers.

3.1 Review of Current NDT Techniques

3.1.1 Acoustic and Ultrasound NDT

Acoustic and ultrasound NDT are based upon elastic wave propagation in solids. Examples include the techniques of pulse-echo, impact-echo, ultrasonic, acoustic emission, and spectral analysis of surface waves (SASW). Disadvantages of acoustic NDT include the need of intimate contact between the equipment and the subject, the use of sound couplant, as well as the existence of multiple paths through the same subject that make result interpretations difficult [20].

3.1.2 Thermal NDT

Thermal NDT is based on the detection of heat flow in the object in which air gaps resulting from debonding act as insulators blocking out the proper heat flow. Data interpretation is, however, complicated because of varying ambient temperature conditions and surface emissivity variations, which is a function of surface properties [21]. An attempt was made [22] to quantify subsurface damages of FRP-bonded concrete using infrared thermography.

3.1.3 Radiography NDT

Radiography NDT uses high frequency electromagnetic radiation (X-rays and Gamma rays) or particular beams (beta rays and neutron radiation) passing through the subject and exposing it onto a film on the other side of the subject. Limitations include the need to access both sides of the subject, the need of safety precautions, long exposure, and two-dimensional (2D) images of three-dimensional (3D) subjects [23].

3.1.4 Radar/Microwave NDT

Radar/microwave NDT uses electromagnetic (EM) wave in probing the target structure for inspection. It has been used extensively for site characterization in geotechnical engineering and for evaluating concrete structures, pavements, and bridge decks. Most radar/microwave NDT techniques used in civil engineering applications operate in the range from VHF (very high frequency) (30MHz ~ 300 MHz) to SHF (super high frequency) (3~30 GHz). Radar NDT relies on the reflected signals from the target for ranging and interpretation, while microwave NDT uses reflected as well as transmitted signals for the same purpose. The wave properties of received radar signals, such as velocity and amplitude, depend on the dielectric properties and geometrical properties (scattering effects) of the target structures. Thus, characteristics of the target structure can be revealed from the received signals. Voids, delaminations, rebars, and material characteristics can be detected and interpreted from the reflected waves. Optimization between penetration depths and detection capability, two inversely related parameters that are dependent on the frequencies and bandwidth of the wave, could be a challenge. Conventional radar often makes use of low frequencies to enhance penetration but with sacrificed detectability. With the proper development of wideband, multi-frequency capability and tomographic imaging techniques, along with measurement of dielectric properties of the subject materials, however, radar can be a powerful tool in assessing structural members that consist of hybrid materials.

Several radar NDT techniques for assessing the condition of FRP-retrofitted/wrapped concrete structures have been reported in the literature [24 ~ 27]. Most of the reported radar NDT techniques for damage detection in concrete and FRP-concrete structures rely on the near-field measurements in which EM waves are essentially cylindrical or spherical. The near-field approach is inherently sensitive to localized defects and damages of the structure since the probing device is placed in a close distance to the surface of the structure. Strong reflection response can also be expected. Advantages of the near-field approach include (i) finer spatial resolution, (ii) less vulnerability to unwanted edge reflection, (iii) small size of probing devices/radiators (e.g., antenna, waveguide), and (iv) simple calibration scheme [28]. Disadvantages of the near-field approach include (i) the constraint of short standoff/inspection distance, (ii) complex

radiation patterns in the near-field region, and (iii) degradation in measurement sensitivity due to the surface roughness of the specimen.

The far-field approach, on the other hand, is not constrained by the requirement of accessibility to the structure, neither easily hampered by the surface condition of the structure. The proposed FAR (far-field airborne radar) NDT technique remedies coarse resolution problem by the integration of inverse synthetic aperture radar (ISAR) measurements and tomographic reconstruction methods. Details of this technique will be provided in the following sections.

3.2 Overview of the FAR NDT Technique

The FAR NDT technique mainly consists of an airborne horn antenna, a signal generator, a signal modulator, and an analyzer. In principle, radar signals are designed and generated by the signal generator, modulated by the modulator, and transmitted by the horn antenna. The horn antenna is placed beyond the far-field distance from the structure. Hence, the impinging radar signals on the structure will be essentially plane waves whose waveform is mathematically simplified for analysis. The inspection scheme is illustrated in Fig. 1 where the radar is positioned at an inclined angle, ϕ, with respect to the horizontal axis (level).
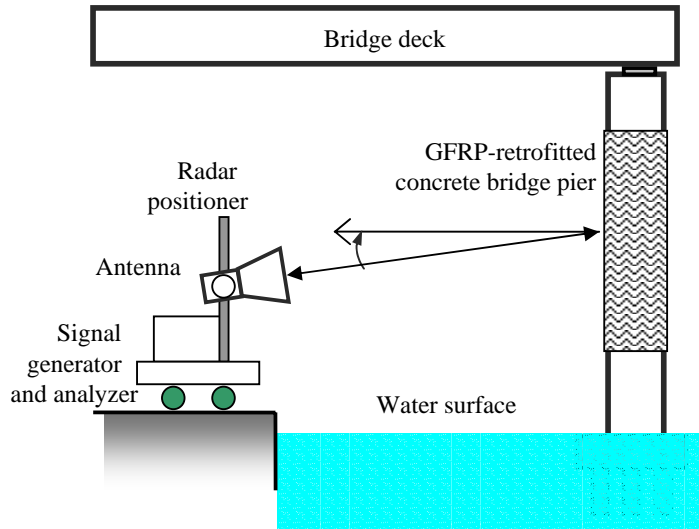

Fig. 1 Inspection scheme of the FAR NDT technique

Continuous wave (CW) radar signals in the frequency range of 8GHz to 12GHz and linearly polarized in HH (transverse electric) and VV (transverse magnetic) were used for the relevance of their wavelengths in matching the typical size of FRP debonding. Reflected EM waves or radar signals are collected by the same horn antenna and processed by the analyzer. The radar measurements are collected in ISAR (inverse synthetic aperture radar) mode; in other words, the reflected signals are received at different angles with respect to the structure. Collected far-field ISAR measurements are represented in dBsm (decibel per square meter) for the amplitude and in radian for the phase. Far-field ISAR radar measurements collected at various angles and frequencies constitute the frequency-angle data for signal processing based on tomographic reconstruction methods. Image reconstruction processing is implemented by fast projection algorithm [29]. Reconstructed imagery is used as a basis for condition assessment.

3.3 Specimen Description and Experimental Measurement

Laboratory GFRP-wrapped concrete cylinders with and without an artificial defect embedded in the interface region between the GFRP layer and the concrete were manufactured and subjected to radar measurements. Two representative GFRP-concrete specimens are shown in Fig. 2. In Fig. 2 (a), the intact concrete cylinder was wrapped with one layer of GFRP after 28 days of curing. The artificial defect made of a cubic-like Styrofoam (3.81cm-by-3.81cm-by-2.54cm) was introduced to the damaged specimen as shown in Fig. 2 (b). The mix ratio of concrete for both specimens was water:cement:sand: aggregate is 0.45:1:2.52:3.21 (by weight). The diameter of concrete cores was 15.2 cm, and the height was 30.4 cm. A unidirectional glass fabric system (Tyfo® SEH-51A by Fyfe Co. LLC) was used and molded with epoxy resin (Tyfo® S Epoxy) to form the GFRP-epoxy sheet wrapped on the surface of the concrete core. The volumetric ratio of epoxy:GFRP was 0.645:0.355. The thickness of the GFRP-epoxy sheet was 0.25 cm.
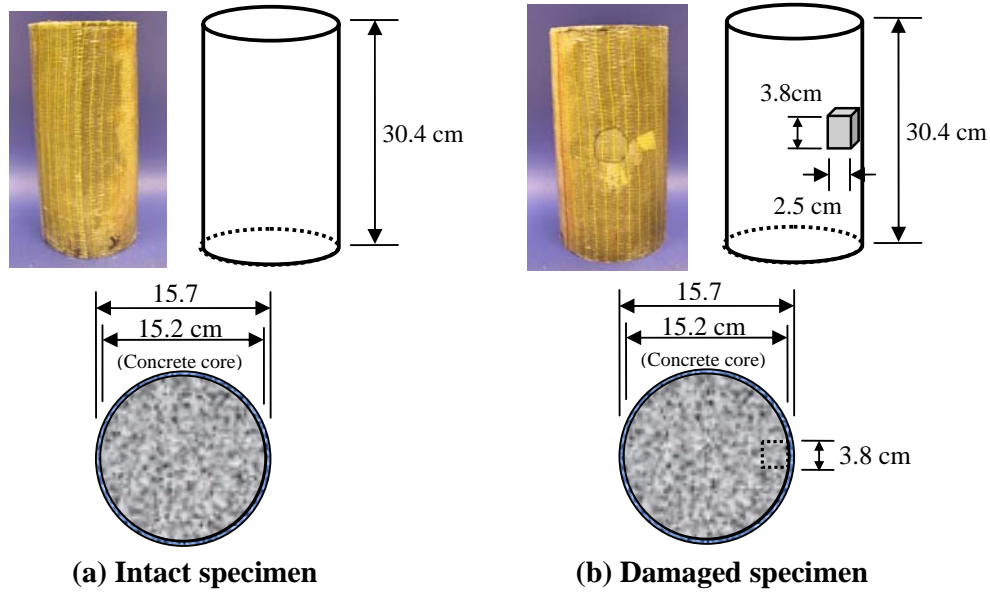
30.4 cm

3.8cm

30.4 cm

2.5 cm

15.7

15.2 cm

(Concrete core)

15.7

15.2 cm

(Concrete core)

3.8 cm

(a) Intact specimen   **(b) Damaged specimen**

Fig. 2 Intact and damaged GFRP-wrapped concrete cylinder specimens

Physical radar measurements of the GFRP-wrapped concrete specimens were performed at the M.I.T. (Massachusetts Institute of Technology) Lincoln Laboratory using the Compact RCS/Antenna Range facility capable of achieving high signal-to-noise ratio measurements for a large frequency bandwidth ranging from UHF (0.7 GHz) to 100 GHz and producing a 20-m quiet zone for different antenna radiation patterns and full polarimetric RCS measurements. Collected far-field ISAR measurements from the intact and the damaged specimens in the frequency range of 8 GHz to12 GHz are provided in Fig. 3 (a) and (b). In Fig. 3 (b), the incident angle of 0-degree corresponds to the center location where the artificial defect is placed. In Fig. 3 (a) and (b), it is found that the presence of the defect produces more scattering of radar signals in the total reflection response of the damaged specimen than the one of the intact specimen. This is especially significant in the angular region other than normal incidence (0-degree case), as observed in Fig. 3 (b).
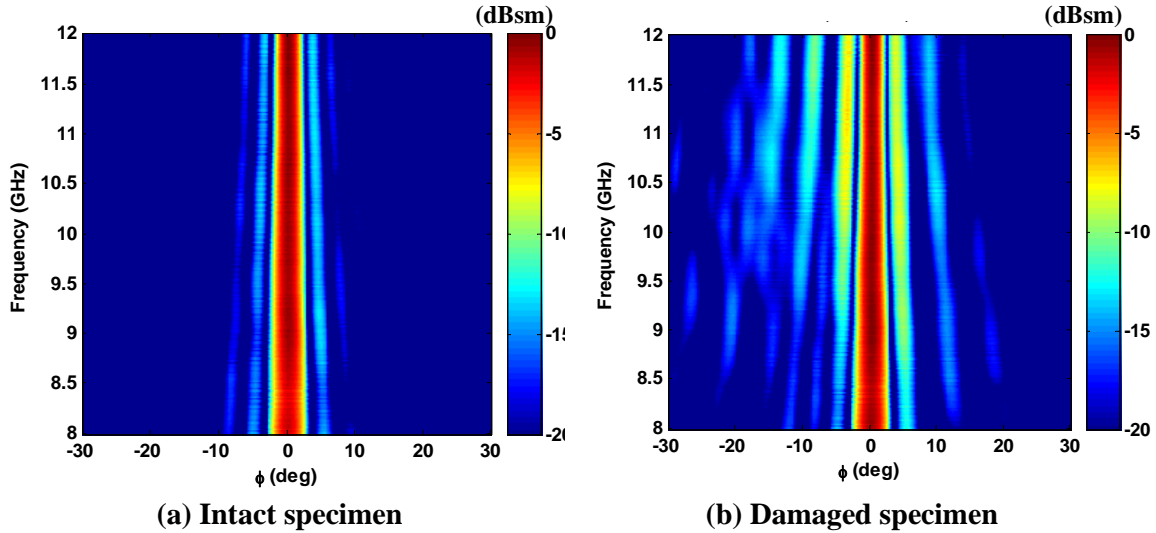
(a) Intact specimen **(b) Damaged specimen**

Fig. 3 Frequency-angle data of the intact and damaged specimens

(HH polarization, 8GHz ~12 GHz)

3.3 Progressive Image Focusing

Image reconstruction is performed through the progressive image focusing in conjunction with the use of far-field ISAR measurements for the intact specimen. In this application, the near-surface artificial defect with characteristic lengths 3.72 cm (range) and 3.76 cm (cross-range) are theoretically detectable beyond a far-field distance 10 m with bandwidth 4 GHz (center frequency 10 GHz) using a horn antenna with aperture size 0.4 m (Fig. 4). The center frequency is shifting with the increasing of bandwidth in Fig. 4. It is shown that, in Fig. 4, the range and cross-range resolutions of the far-field ISAR measurements are dramatically improved with increasing bandwidth.
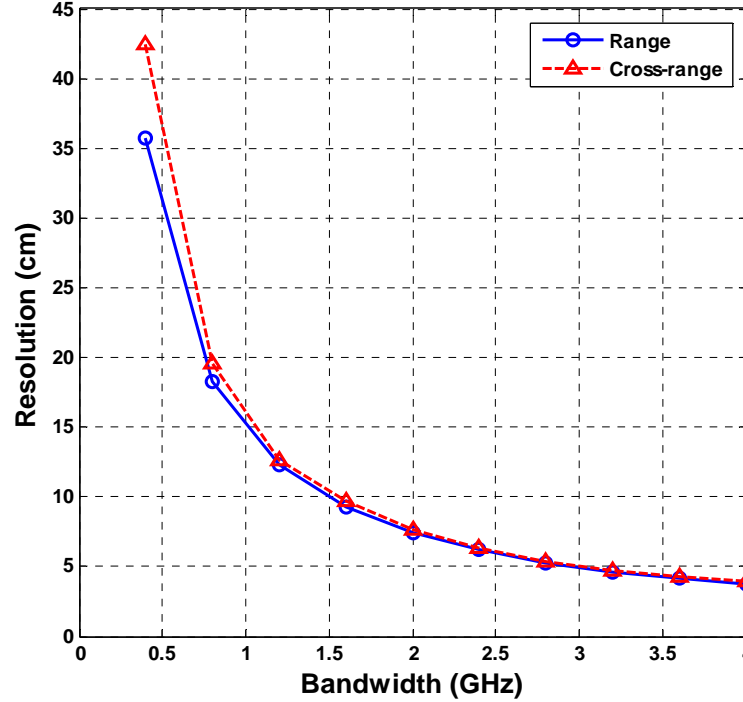
Fig. 4 Range and cross-range resolutions versus bandwidth – shifting center frequency

The measurements are processed to render the images as shown in Fig. 5. Bandwidth of each image is increased from the upper left image (0.44 GHz) to the lower right image (4 GHz), with frequency band indicated in each image. In Fig. 5, the features of the specimen are gradually revealed by the converging of scattering signals in the images. Two scattering signals representing the effect of the two ends of the specimen are identified in the upper middle image with bandwidth 0.88 GHz. This feature becomes clearer in other images with wider bandwidths.

Although 4GHz bandwidth is presumably suggested, geometric features of the specimen are visually detectable when the bandwidth is only about 1 GHz. This implies that, by taking the advantages of ISAR measurement and fast backprojection algorithm, the ability of the imagery to capture the features of the target structure can be increased if *a priori* knowledge on the shape and size of the target structure is available. This is the case for preliminary inspection where the global features would be first revealed at narrow bandwidths. Therefore, the detection ability of the imagery is believed to be higher than theoretical values as

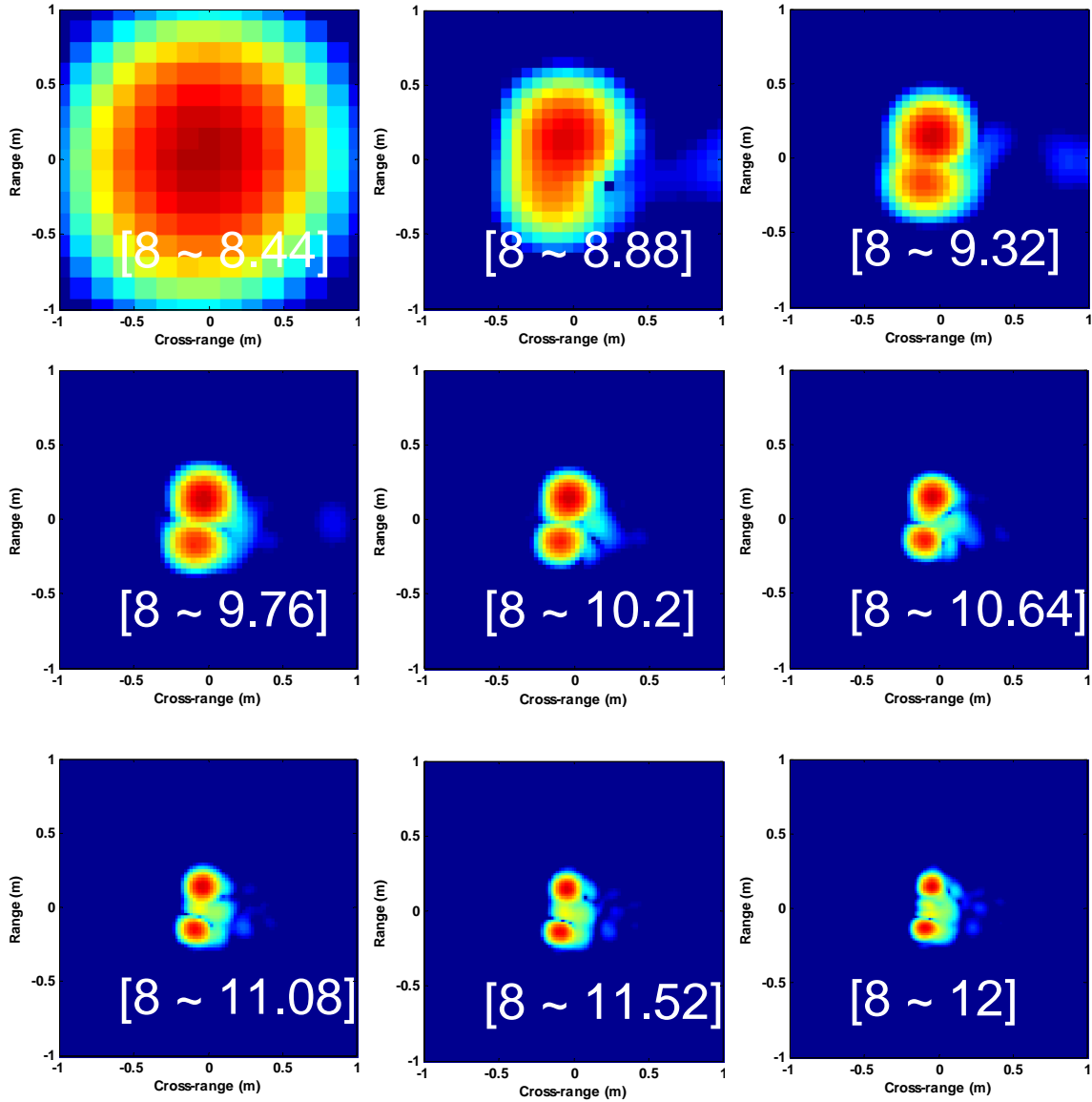shown in Fig. 5. This feature also makes the proposed radar NDT technique promising for in-field applications.

Fig. 5 Processed images of the intact specimen with various bandwidths

3.5 Image Reconstruction for Structural Assessment

3.5.1 Damage Detection

Damage detection for the structural assessment of GFRP-wrapped concrete systems is conducted by interpreting scattering signals in the reconstructed images. To demonstrate this, reconstructed images of the intact and the damaged GFRP-wrapped concrete specimens using the far-field ISAR measurements (Fig. 3) are rendered and shown in Figs. 6 and 7, respectively. In these figurs, the specimen boundaries are indicated in solid lines. In Fig. 6, the reconstructed scattering signals are only due to the edge or surface reflection. On the other hand, in Fig. 7, the reconstructed image reveals not only the edge reflections but also the presence of the defect. In other words, the presence of the artificial defect is detected and represented by the scattering signal in the middle of the specimen in Fig. 7 ($\phi = 10°$).

Knowing the nature of these scattering signals and the geometry of the structure, image interpretation can be performed for damage detection. Factors such as incident angle, bandwidth, and center frequency are to be discussed for their effects on the performance of image interpretation in the following sections.
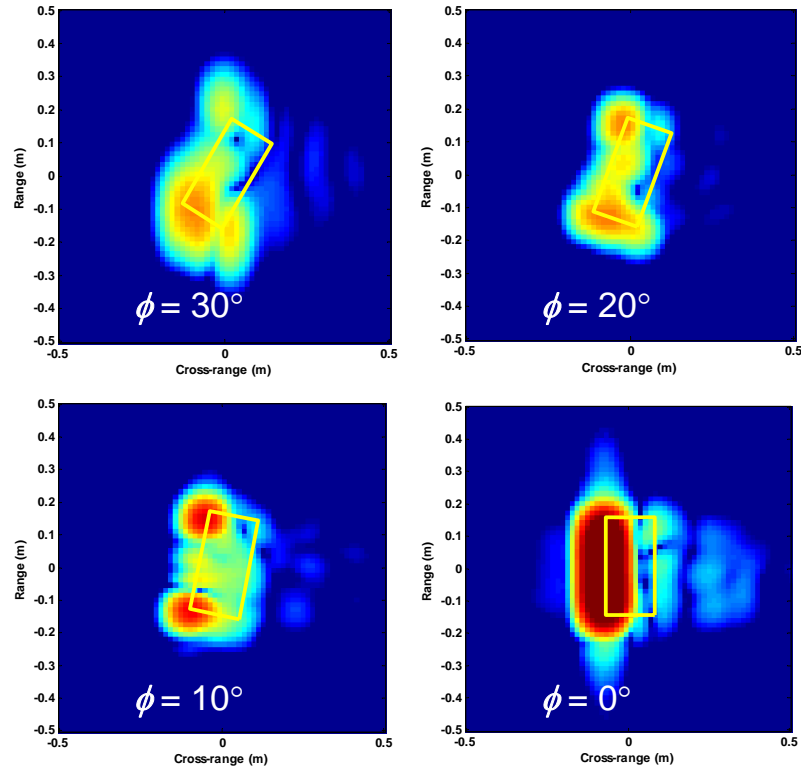
Fig. 6 Reconstructed images of the intact GFRP-concrete specimen ($\phi = 30° \sim 0°$)

3.5.2 Effectiveness of Incident Angle

In the reconstructed images, significant scattering signals are encountered when reflected signals due to the presence of defects are strong, except in the normal incidence (or specular return) case ($\phi = 0°$). Excluding the scattering signals due to edge reflection and specular return, the stronger the scattering signal is, the more affirmative there is a defect.

Since defects can always be implicitly or explicitly characterized by their orientation, certain ranges of incident angle can be more effective than others in revealing or triggering the scattering signals due to defects. It is shown that, in Fig. 7, the defect indication is most obvious when $\phi = 10°$ among other angles.
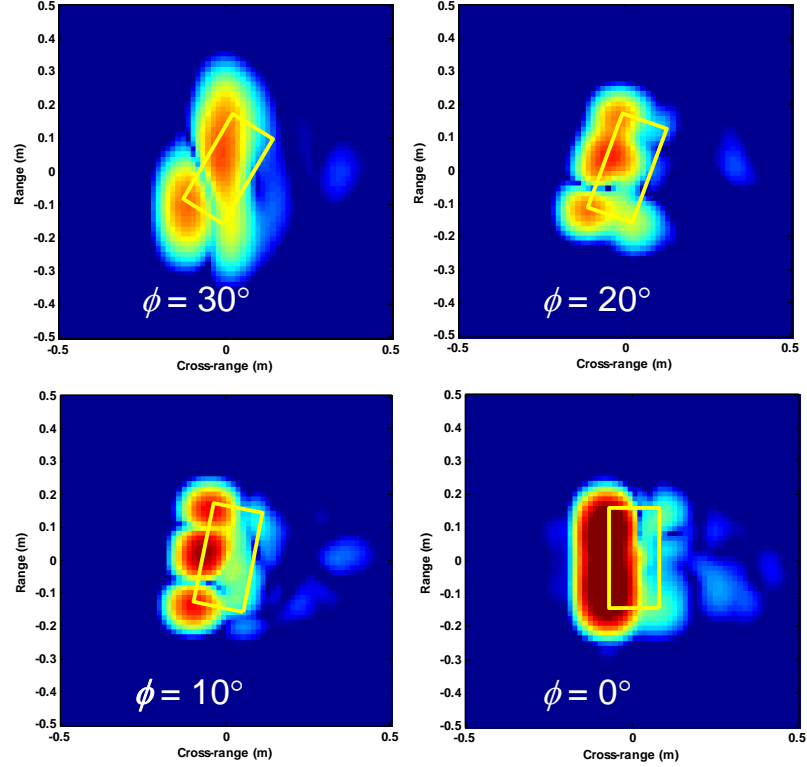
16

Fig. 7 Reconstructed images of the damaged GFRP-concrete specimen ($\phi = 30° \sim 0°$)

3.5.3 Effects of Bandwidth and Center Frequency

As shown in Fig. 5, the increase of bandwidth in image reconstruction processing leads to the improvement of image resolutions. Such increase can be associated with constant center frequency or shifting center frequency (Fig. 8). The example in Fig. 5 uses shifting center frequency. The use of constant center frequency results in the resolution versus bandwidth relationship as shown in Fig. 9.
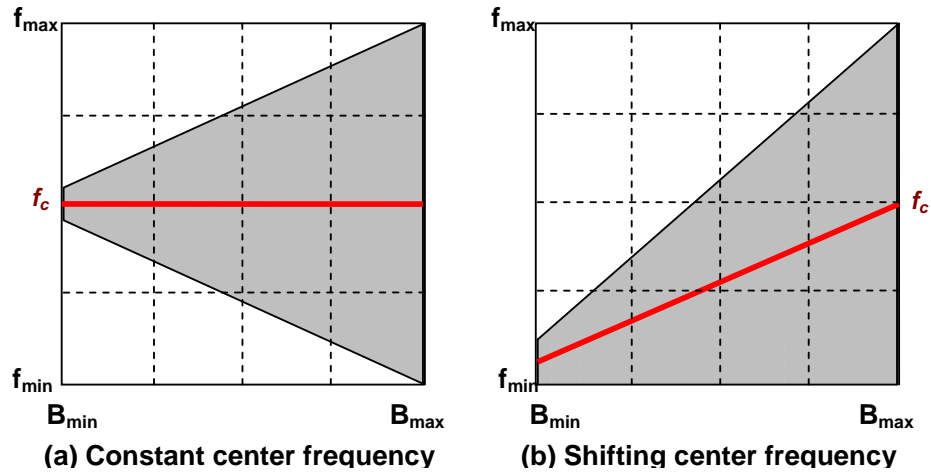
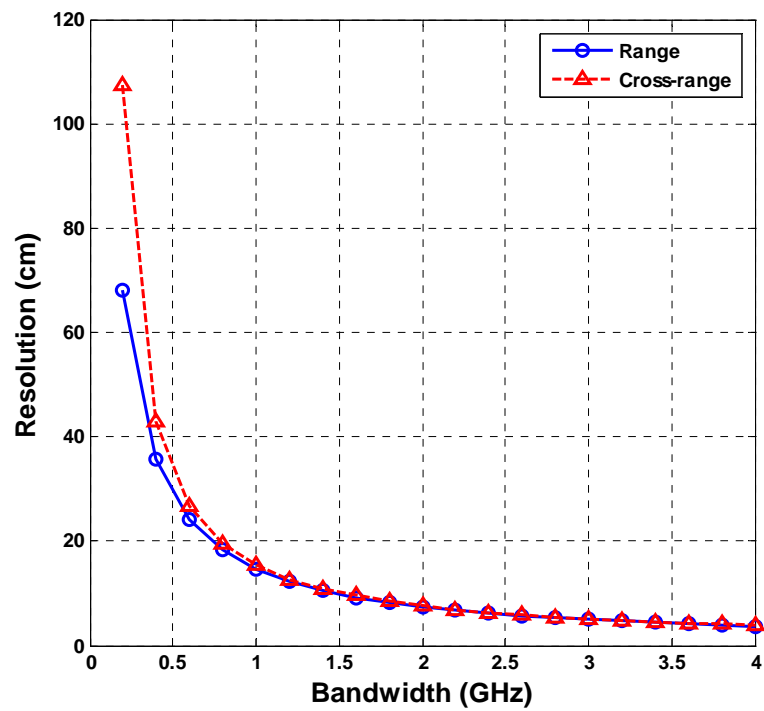**Fig. 8** Constant and shifting center frequency schemes

Fig. 9 Range and cross-range resolutions versus bandwidth – constant center frequency

Comparison of Fig. 5 (shifting center frequency) and Fig. 9 (constant center frequency) shows the improvement of the rate of range and cross-range resolutions using shifting center frequency. This is because shifting center frequency scheme has more complete frequency content than the constant scheme. This observation also suggests a continuous exploration in the frequency band and an increasing use of bandwidth for processing.

4 Summary

The developed FAR NDT technique for the structural assessment of GFRP-wrapped concrete structures mainly consists of two components: (1) far-field ISAR measurements, and (2) image reconstruction algorithm. In this paper, work is reported on laboratory radar measurements of GFRP-concrete specimens in the far-field region at different angles in the frequency range of 8GHz to 12GHz. The measured frequency-angle data are processed by the imaging algorithm (fast backprojection algorithm) to reconstruct the range-cross-range imagery of the structure for structural assessments.

The presence of the artificial defect is detected and represented by the scattering signal in reconstructed images, as demonstrated in this paper. Progressive image focusing based on fast projection algorithm provides a capability for various purposes of inspection in field applications. Image reconstruction using shifting center frequency is proved to be more efficient than using constant center frequency scheme. In the FAR NDT technique, the increase of bandwidth implemented in image reconstruction significantly improves the image resolutions. The detectability of defects is sensitive to the selection of incident angle. Further research is needed to quantitatively define the relationship between the detectability of defects and the incident angle. From the results presented in this paper, it is believed that the developed FAR NDT capability is applicable for the field inspection of GFRP-wrapped concrete bridge piers in prevention of collapse.

Acknowledgement

References

[1] Au C, Büyüköztürk O (2005) Effect of fiber orientation and ply mix on fiber reinforced polymer-confined concrete. J Compos Constr 9(5):397-407.

[2] Sheikh SA, Yau G (2002) Seismic behaviour of concrete columns confined with steel and fibre reinforced polymers. ACI Struct J 99 (1):72-80.

[3] Au C, Büyüköztürk O (2006) Peel and shear fracture characterization of debonding in FRP plated concrete affected by moisture. J Compos Constr 10(1):35-47.

[4] Buyukozturk O, Gunes O, Karaca E (2004) Progress on understanding debonding problems in reinforced concrete and steel members strengthened using FRP composites. Constr Build Mater 18:9-19.

[5] Teng JG (2006) Debonding failures of RC beams flexurally strengthened with externally bonded FRP reinforcement. In: Proceedings of Eleventh International Conference and Exhibition of Structural Faults + Repair 2006, University of Edinburgh, Scotland, UK.

[6] Büyüköztürk O, Yu T-Y (2006) Understanding and assessment of debonding failures in FRP-concrete systems. In: Proceedings of Seventh International Congress on Advances in Civil Engineering. Yildiz Technical University, Istanbul, Turkey.

[7] Büyüköztürk O, Hearing B, Gunes O (1999a) Performance and durability related issues in retrofitting concrete members with FRP. In: Proceedings of the 13th ASCE Engineering Mechanics Division Conference, June 13-16, The John Hopkins University, Baltimore, MD.

[8] Smith ST, Teng JG (2001) Interfacial stresses in plated beams. Eng Struct 23(7):857-871.

[9] Leung CKY (2001) Delamination failure in concrete beams retrofitted with a bonded plate. ASCE J Mater Civil Eng 13(2):106-113.

[10] Chajes MJ, Thompson TA, Farschman CA (1995) Durability of concrete beams externally reinforced with composite fabrics. Constr Build Mater 9(3):141-148.

[11] Toutanji H, Gomez W (1997) Durability characteristics of concrete beams externally bonded with FRP composite sheets. Cement Concrete Compos 19(4):351-358.

[12] Karbhari VM, Zhao L (1998) Issues related to composite plating and environmental exposure effects on composite-concrete interface in external strengthening. Compos Struct 40(3-4):293-304.

[13] Green MF, Bisby LA, Beaudoin Y, Labossiere P (2000) Effect of freeze-thaw cycles on the bond durability between fibre reinforced polymer plate reinforcement and concrete. Canadian J Civil Eng 27(5):949-959.

[14] Hamilton HR III (2000) Durability of FRP reinforcements for concrete. Progress Struct Eng Mater 2:139-145.

[15] Di Tommaso A, Neubauer U, Pantuso A, Rostasy FS (2001) Behavior of adhesively bonded concrete-CFRP joints at low and high temperatures. Mech Compos Mater 37(4):327-338.

[16] Kinloch AJ (1982) The science of adhesion. J Mater Sci 17(3):617-651.

[17] Antoon MK, Koenig JL (1980) The structure and moisture stability of the matrix phase in glass- reinforced epoxy composites. J Macromolecul Sci – Rev Macromolecul Chem C19(1):135-173.

[18] Hutchinson AR (1986) Durability of structural adhesive joints. Ph.D. Thesis, Dundee University, UK.

[19] Yu T-Y, Buyukozturk O (2007) A Far-field airborne radar NDT technique for debonding and rebar detection in GFRP-retrofitted concrete structures, NDT&E Intl (in press).

[20] Hillger W (1987) Inspection of concrete by ultrasonic testing. In: Proceedings of the 4th European Conference on Non-Destructive Testing. London UK, 2:1003-1012.

[21] de Vekey RC (1990) Non-destructive evaluation of structural concrete: a review of European practice and developments. In: Proceedings of Nondestructive Evaluation of Civil Structures and Materials. Boulder, CO.

[22] Starnes MA, Carino NJ, Kausel EA (2003) Preliminary thermography studies for quality control of concrete structures strengthened with fiber-reinforced polymer composites. ASCE J Mater Civ Eng 15(3):266-273.

[23] Malhotra VM, Carino NJ (1991) CRC handbook on nondestructive testing of concrete. CRC Press, Boca Raton, FL.

[24] Li J, Liu C (2001) Noncontact detection of air voids under glass epoxy jackets using a microwave system. Subsurf Sens Tech Appl 2(4):411-423.

[25] Feng MQ, De Flaviis F, Kim YJ (2002) Use of microwave for damage detection of fiber reinforced polymer-wrapped concrete structures. J Eng Mech 128(2):172-183.

[26] Kim YJ, Jofre L, De Flaviis F, Feng MQ (2003) Microwave reflection tomographic array for damage detection of civil structures. IEEE Trans Antennas Prop 51(11):3022-3032.

[27] Akuthota B, Hughes D, Zoughi R, Myers J, Nanni A (2004) Near-field microwave detection of disband in carbon fiber reinforced polymer composites used for strengthening cement-based structures and disbond repair verification. J Mater Civil Eng 16(6):540-546.

[28] Zoughi R, Lai J, Munoz K (2001) A brief review of microwave testing of stratified composite structures: A comparison between plane wave and near-field approaches. Mater Eval 60(2):171-177.

[29] Yegulalp AF (1999) Fast backprojection algorithm for synthetic aperture radar. In: Proceedings of IEEE Radar Conference, 20-22 April:60-65.